ARMY RESEARCH LABORATORY

The Response of Small Scale Rigid Targets to Shallow Buried Explosive Detonations

D. M. Fox, X. Huang, D. Jung, W. L. Fourney, U. Leiste, and J. S. Lee

ARL-RP-339 **September 2011**

A reprint from the *International Journal of Impact Engineering*, Vol. 38, pp. 882–891, 2011.

NOTICES

Disclaimers

The findings in this report are not to be construed as an official Department of the Army position unless so designated by other authorized documents.

Citation of manufacturer's or trade names does not constitute an official endorsement or approval of the use thereof.

Destroy this report when it is no longer needed. Do not return it to the originator.

Army Research Laboratory
Aberdeen Proving Ground, MD 21005-5066

ARL-RP-339 **September 2011**

The Response of Small Scale Rigid Targets to Shallow Buried Explosive Detonations

D. M. Fox and X. Huang
Weapons and Materials Research Directorate, ARL

D. Jung, W. L. Fourney, and U. Leiste
University of Maryland

J. S. Lee
Yonsei University

A reprint from the *International Journal of Impact Engineering*, Vol. 38, pp. 882–891, 2011.

REPORT DOCUMENTATION PAGE

Form Approved
OMB No. 0704-0188

1. REPORT DATE *(DD-MM-YYYY)*	2. REPORT TYPE	3. DATES COVERED (From - To)
September 2011	Reprint	18 June 2010–18 May 2011

4. TITLE AND SUBTITLE
The Response of Small Scale Rigid Targets to Shallow Buried Explosive Detonations

5a. CONTRACT NUMBER

5b. GRANT NUMBER

5c. PROGRAM ELEMENT NUMBER

6. AUTHOR(S)
D. M. Fox, X. Huang, D. Jung,[*] W. L. Fourney,[*] U. Leiste,[*] and J. S. Lee[†]

5d. PROJECT NUMBER

5e. TASK NUMBER

5f. WORK UNIT NUMBER

7. PERFORMING ORGANIZATION NAME(S) AND ADDRESS(ES)
U.S. Army Research Laboratory
ATTN: RDRL-WMF-F
Aberdeen Proving Ground, MD 21005-5066

8. PERFORMING ORGANIZATION REPORT NUMBER
ARL-RP-339

9. SPONSORING/MONITORING AGENCY NAME(S) AND ADDRESS(ES)

10. SPONSOR/MONITOR'S ACRONYM(S)

11. SPONSOR/MONITOR'S REPORT NUMBER(S)

12. DISTRIBUTION/AVAILABILITY STATEMENT
Approved for public release; distribution is unlimited.

13. SUPPLEMENTARY NOTES
A reprint from the *International Journal of Impact Engineering*, Vol. 38, pp. 882–891, 2011.
[*]Department of Mechanical Engineering, University of Maryland, College Park, MD 20742
†Department of Mechanical Engineering, Yonsei University, Seoul, Republic of Korea

14. ABSTRACT
Experimental and computational investigations were performed in order to better understand the mechanical response of rigid targets with various geometries to the detonation of shallow buried explosives. The motion of the targets was measured by use of high-speed digital video photography. This work involved flat targets, targets that were downwardly convex, and targets that were downwardly concave with explosive charges located at various positions beneath the targets. It was observed that, in general, angled hulls – whether downwardly concave or convex – tended to reduce the amount of momentum imparted to the center of mass of the targets. Computations were performed by use of an arbitrary Langrangian–Eulerian treatment in a nonlinear finite element code. A model based on quasistatic test evaluations of wet concrete sand was used for prediction of the soil behavior. The computational technique provided very good agreement between computation and experiment.

15. SUBJECT TERMS
mine blast, shallow buried explosive, small-scale experiments, soil model, computation mechanics, arbitrary Lagrangian-Eulerian method

16. SECURITY CLASSIFICATION OF:			17. LIMITATION OF ABSTRACT	18. NUMBER OF PAGES	19a. NAME OF RESPONSIBLE PERSON
a. REPORT	b. ABSTRACT	c. THIS PAGE			David M. Fox
Unclassified	Unclassified	Unclassified	UU	16	19b. TELEPHONE NUMBER (*Include area code*) 410-278-6033

International Journal of Impact Engineering 38 (2011) 882–891

Contents lists available at ScienceDirect

International Journal of Impact Engineering

journal homepage: www.elsevier.com/locate/ijimpeng

The response of small scale rigid targets to shallow buried explosive detonations

D.M. Fox [a,c], X. Huang [a], D. Jung [b], W.L. Fourney [b], U. Leiste [b], J.S. Lee [d,*]

[a] Blast Protection Branch, Army Research Laboratory, Aberdeen, Proving Ground, MD 21005 5066, USA
[b] Department of Mechanical Engineering, University of Maryland, College Park, MD 20742, USA
[c] Department of Mechanical Engineering, Wayne State University, Detroit, MI 48202, USA
[d] Department of Mechanical Engineering, Yonsei University, Seoul, Republic of Korea

ARTICLE INFO

Article history:
Received 18 June 2010
Received in revised form
11 May 2011
Accepted 18 May 2011
Available online 12 June 2011

Keywords:
Mine blast
Small-scale experiments
Soil model
Computational mechanics
Arbitrary Lagrangian–Eulerian method

ABSTRACT

Experimental and computational investigations were performed in order to better understand the mechanical response of rigid targets with various geometries to the detonation of shallow buried explosives. The motion of the targets was measured by use of high-speed digital video photography. This work involved flat targets, targets that were downwardly convex, and targets that were downwardly concave with explosive charges located at various positions beneath the targets. It was observed that, in general, angled hulls – whether downwardly concave or convex – tended to reduce the amount of momentum imparted to the center of mass of the targets. Computations were performed by use of an arbitrary Langrangian–Eulerian treatment in a nonlinear finite element code. A model based on quasi-static test evaluations of wet concrete sand was used for prediction of the soil behavior. The computational technique provided very good agreement between computation and experiment.

1. Introduction

Physical tests involving full-scale vehicle systems subjected to blast loads are relatively expensive. The judicious development and implementation of properly conceived experimental, computational and analytical methods to better illustrate the mechanics of mine blast phenomena can be used to significantly reduce the scale and cost of experimentation and thus moderate the cost of development of mine protected vehicles and protective equipment for infantry and demining personnel. One area of active investigation relates to the manner in which shallow buried explosives excite mechanical structures.

Numerous experimental techniques, analytical methods, and correlations for the description of blast events and for the prediction of structural response to blast inputs have been developed over the years. Baker [1] assembled an excellent review of experimental and theoretical results relating to air blast. Kinney and Graham [2] collected and compiled air blast data from various sources. Based on these data, they showed empirical formulations for the prediction of air blast phenomena. Westine et al. [3] performed tests with measurement of impulse imparted to flat plates from explosives buried in soil and, based on the results, developed an empirical correlation for the prediction of structural excitation from blasts from shallow buried explosives.

It has been shown that small-scale experimental results can closely match those for full-scale tests. In the work reported by Fourney et al. [4] and Taylor et al. [5,6], results from full-scale blast tests involving explosives buried to shallow depths in wet concrete sand were compared with results for small-scale predictive tests. The full-scale test series was conducted with plates weighing up to 12,700 kg and using up to 4.54 kg of TNT. For the work reported by Fourney et al. [4], small-scale charge sizes of 203 mg, 609 mg, and 3.3 g were used to predict impulse and help design the full-scale tests. The small-scale results were used to predict what would happen using full-scale charge sizes of either 2.27 or 4.54 kg. For the full-scale tests the stand off distance was varied between zero (plate on the ground) and 0.4064 m. Depth of burial for the full-scale tests was varied between 0.0806 and 0.3048 m. It was concluded, based on the test data reported that small-scale tests, by means of Hopkinson–Cranz scaling, could be used very effectively to predict target impulse for full scale tests.

Genson [7] performed small-scale blast tests on rigid aluminum plates with variously shaped bottoms – some were flat and others were v-shaped and downwardly convex – in order to explore the nature of the impulse applied to these targets as a function of target geometry, depth of explosive burial, and stand off distance between the target and the ground. For these investigations, the explosive charge was buried in wet concrete sand and was located directly

* Corresponding author. Tel.: +82 2 2123 5820; fax: +82 2 312 2159.
E-mail address: joonlee@yonsei.ac.kr (J.S. Lee).

0734-743X/$ – see front matter © 2011 Elsevier Ltd. All rights reserved.
doi:10.1016/j.ijimpeng.2011.05.009

underneath the center of the plates. That work showed that as the angle of downwardly convex v-shaped hulls increased, impulsive loads imparted to them were reduced. Increased depth of burial, until a region of asymptotic response was reached, intensified the loading to the plate while increasing the distance between the ground surface and the target served to reduce the impulse supplied to the target.

Various researchers have applied computational techniques for treatment of the behavior of explosive, soil, and target in mine blast situations. Laine and Sandvik [8] developed a constitutive model that has been used as the basis for definition of the behavior of sand. Szymzcak [9] applied a viscoplastic model for soil and used a generalized hydrodynamic numerical formulation in order to predict the response of flat plates to excitation from explosives buried in wet sand. It was observed that this computational approach matched experimental results very well as long as the ratio of target height above the ground to depth of burial was three or less. Grujicic et al. [10,11] have investigated the use of various soil constitutive models with incorporation of porosity effects. More recently, Deshpande et al. [12] have proposed a novel approach to modeling the soil that takes into account various regimes of soil behavior that evolve during the course of the detonation event.

Neuberger et al. [13] examined the scaling of flat plate deformation with excitation from large explosive charges flush buried in dry sand, by means of a combination of experiment and computation. The computation agreed well with experiment and was performed using an arbitrary Langrangian–Eulerian technique with the dry sand modeled by means of a generalized Mohr–Coulomb model. The computational and experimental results supported a hypothesis that the blast response of targets to detonation of large explosives flush buried in dry sand would follow a scaling relation.

Williams et al. [14] used a Lagrangian method, with soil and explosive modeled with a particle technique and soil behavior prescribed using a hybrid elastic–plastic model, to predict the response of a flat target to the blast from a shallow buried explosive. Three types of soil were modeled – dry sand, a mix of clay and sand, and a wet clay – and although direct correlations to experiment were not presented, computational results followed the expected trend, viz., the impulse imparted to the target increased with decreasing soil compressibility and yield strength.

Results that involve the loading imparted, by means of explosive shallow buried in wet sand, to flat targets, downwardly concave targets, and downwardly convex targets are examined. The effect of variation of explosive lateral location relative to the centerline of the targets is also examined, as is the effect of variation of the angle of concavity and convexity. Impulse response for downwardly concave models is compared with the response for downwardly concave targets in order to further investigate the question of whether the well known reduction in impulse for the downwardly convex topology is altogether due merely to an increased offset of target bottom surface from the soil surface.

Although accurate analytical and computational techniques for predicting air blast loading have been available for many years, methods for calculation of the impulse propagated from shallow buried explosive still offer opportunities for improvement. We will present a synthesis of computational techniques that shows a great deal of promise with regard to an accurate definition of blast threats involving explosives that are shallow buried in various types of soil.

2. Experimental procedures

As discussed in the Introduction, above, the charge size and scale of the present work has been found to be easy to manage and to be appropriate for prediction of full-scale tests. Fig. 1 illustrates the

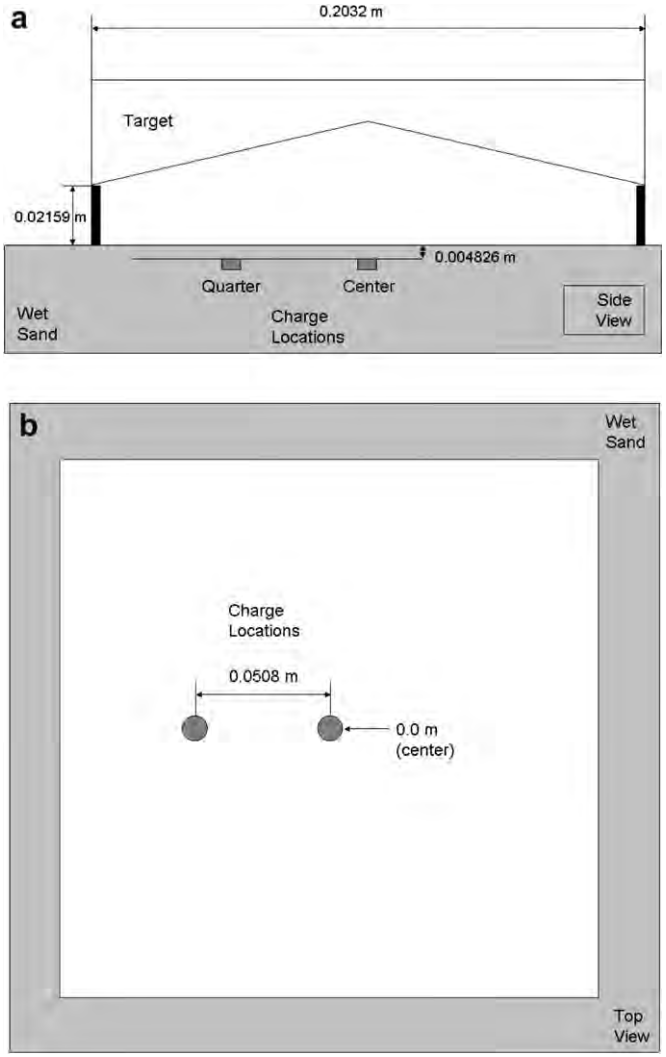

Fig. 1. Experimental setup. A total of 0.636 g cylindrical explosive charges were buried to a depth of 4.826 mm in wet concrete sand and placed at various distances from the centerline of rigid aluminum targets. The vertical distance between the top surface of the sand and the lowest point of each of the 203.2 mm × 203.2 mm targets was 21.59 mm. Each test performed was a specific combination of one target geometry and one charge location. a. Side view. b. Top view.

experimental setup used to measure the response of the rigid aluminum plates to the excitation of shallow buried explosive. The 636 mg explosive charges used for this work were constructed with of Detasheet C, which contributed 567 mg of the high explosive PETN, and an RP-87 detonator, which added another 26 mg of PETN and 43 mg of RDX so that the total amount of explosive added by the detonator was 69 mg. Most of the mechanical energy from the detonation was, therefore, provided by the Detasheet C. The cylindrical charges were inserted into a bed of wet concrete sand in such a way that their top faces were 4.826 mm below the top surface of the sand. The rigid aluminum target plates were located in the desired conformation above the buried charge. The lowest point of each plate was positioned at the desired stand off distance, 21.59 mm, above the surface of the sand using either blocks of wood or stand off bolts. The experimental work performed for the present study builds upon the initial work done by Genson [7], but includes a deeper investigation of the effects of variation of charge location and target shape. In fact, the fine details regarding test bed preparation, explosive charge manufacture, and most aspects of the experimental procedures performed for the present work are contained in Genson. The charge

size, depth of burial of the explosive, and distance from the soil surface to the bottom of the target would be expected to compare, using Hopkinson–Cranz scaling, with a full-size charge of 4.54 kg, a full-size depth of burial of 93 mm, and a full-size distance from soil surface to target bottom of 416 mm.

The displacements of markings on the corners of each of the plates were measured by use of high-speed digital video. These displacement measurements were used to calculate the velocities of the plates. The velocity values, in conjunction with the measured masses of the targets were then used to determine the impulse imparted to the targets. Fig. 2 shows the geometries of the plates that were tested. The plates were constructed of aluminum alloy 6061 and behaved essentially as rigid bodies in their response to the loading from the buried explosive. The plates were machined in such a way that all of them were of, nominally, 1.5 kg mass. The particle size distribution for the concrete sand that was used was determined experimentally using a sieve test and is shown in Fig. 3.

3. Computational procedures

Given a moving mesh, the conservation equations, neglecting thermal effects, for the transport of mass, momentum, and energy, respectively, are:

$$\frac{\partial \rho}{\partial t} = -\rho v_{i,i} - (v_i - u_i)\rho_{,i} \tag{1}$$

$$\rho \frac{\partial v_i}{\partial t} = t_{ji,j} + \rho b_i - \rho(v_i - u_i)v_{j,i} \tag{2}$$

$$\rho \frac{\partial e}{\partial t} = t_{ij}d_{ij} + \rho b_i v_i - \rho(v_i - u_i)e_{,i} \tag{3}$$

where ρ is the mass density, u_i the mesh velocity vector, v_i the material velocity vector, t_{ij} the stress tensor, b_i the body force vector, e the internal energy, d_{ij} the rate of deformation tensor, and where, for any quantity Q,

$$Q_{,i} \equiv \frac{\partial Q}{\partial x_i} \tag{4}$$

Computations involving the explosive detonation products, air, and soil were performed by means of a multi-material arbitrary Lagrangian–Eulerian technique as implemented in the LS-DYNA explicit finite element solver [15]. LS-DYNA version 971 R4.2.1 was used for this work. The fluid materials and the aluminum targets were fully coupled by means of a penalty method.

For each time step, a split operator technique was used by the solver to simulate the mass, momentum, and energy transport for the air, detonation product, and soil constituents of the problem. First, there was a Lagrangian step that involved an explicit finite element approach to the solution of the conservation equations. Subsequently a new, more uniform, mesh was created by the solver and then, finally, for each time step, momentum, mass, and energy for each species were advected from the Lagrangian mesh into the new mesh. The donor cell algorithm, a first order upwind scheme, was used to perform the advection step [16].

By means of the multi-material technique within LS-DYNA, it was possible for each element to be populated with more than one material. For each time step, the strain rate for each element was constant and the stress state of each element was determined by summing the products of the volume fraction and stresses of each constituent of the element. Also, for each time step, integration was performed explicitly using central differences.

The interface between the rigid target and the fluids was treated as having infinite slip. At the outer surfaces of the computational domain the default zero force boundary condition was used. For this boundary condition, outflow is not prevented and inflow to cells is constrained to be composed of the same material that is present in the cells [17].

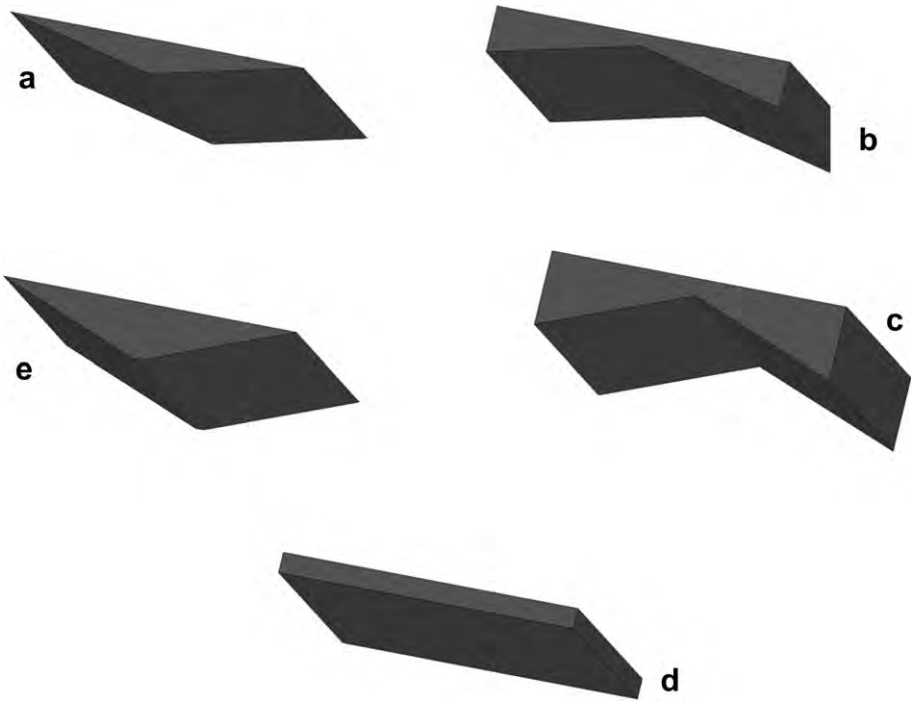

Fig. 2. Target plate geometries, clockwise from top left, (a) 13° convex down; (b) 13° concave down; (c) 21° concave down; (d) flat; and (e) 21° convex down. Targets were machined from aluminum alloy 6061 and shallow buried explosives were detonated at various locations beneath the targets. Target angle was defined as the initial angle between a target bottom half-surface and the horizontal plane.

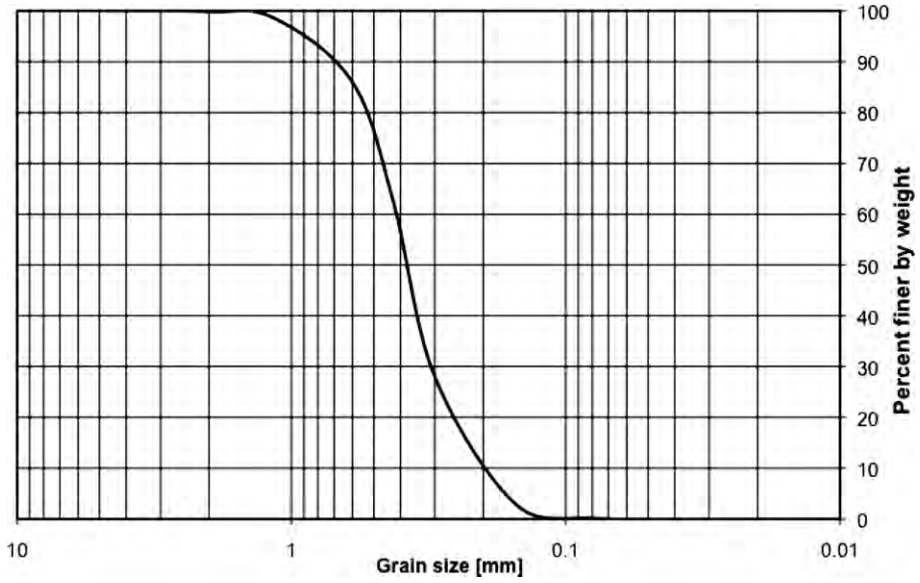

Fig. 3. Particle size distribution for concrete sand.

The 6061 aluminum alloy that comprised the targets was modeled as a rigid solid. The behavior of the reaction products from the detonation of Detasheet C, the high explosive used for this work, was defined in terms of initial density, Chapman–Jouget pressure, detonation velocity, and a Jones Wilkins Lee (JWL) equation of state for description of the adiabat. The form of the JWL equation of state that was used for this work was

$$p = A\left(1 - \frac{\omega}{R_1 V}\right) e^{-R_1 V} + B\left(1 - \frac{\omega}{R_2 V}\right) e^{-R_2 V} + \frac{\omega E'}{V} \tag{5}$$

V in this equation is defined as the ratio of the volume of the detonation reaction products to the initial volume of the explosive; E' is the energy per unit volume; p is the pressure. A, ω, R_1, B, and R_2 are constants available along with the Chapman–Jouget parameters, for many explosives, from various sources. The air was modeled as a fluid with Newtonian viscosity and an ideal gas equation of state

$$p = \rho(C_p - C_v)T \tag{6}$$

where ρ the density, and T the absolute temperature. C_p and C_v, represent the specific heat at constant pressure and at constant volume, respectively.

The behavior of shallow buried explosives in soil is dependent not only on the characteristics of the high explosive but is also very much a function of the properties and moisture content of the soil in which the explosives are buried. The definition of the soil properties as applied in this work was based on some of the standard definitions of soil constitutive properties as found in, e.g., Chen and Baladi [18], and generated for the work that was done to develop hybrid elastic–plastic soil models that were implemented for use in the SABER code, developed by the US Engineer Research and Development Center in conjunction with Titan Research and Technology, for the prediction of ground shock [19]. Equation of state and failure relations were developed for the SABER code based primarily on high pressure, quasi-static test results. One of the objectives of the present work was to test the hypothesis that a soil model based purely on quasi-static tests would be capable of predicting blast loads imparted from shallow buried explosives to rigid targets.

The equation of state, failure surface, and other physical soil parameters used for this work were developed using an iterative linear interpolation process. Starting with the available material parameters from physical tests for concrete sand with 1 and 5 percent air filled voids, LS-DYNA material model 078, *MAT_SOIL_CONCRETE was used to calculate impulsive loading for the flat, center-loaded target using the LS-DYNA ALE technique for each of the two levels of porosity. Subsequently a simple bisection method was used to iteratively perform linear interpolation of all soil model constants until the LS-DYNA impulse result converged to the experimental impulse value and the set of soil material parameters obtained thereby was used to perform computations for all of the other combinations of target geometry and loading configuration. The 1 percent air filled voids concrete sand had a moisture content of 18.2 percent and a dry density of 1790 kg/m^3. The 5 percent air filled voids concrete sand had a moisture content of 16.0% and a dry density, also, of 1790 kg/m^3.

The deviatoric, perfectly plastic failure surface of the soil model used, in tabular form, to populate the LS-DYNA soil model is shown in Fig. 4a. II_s is the second invariant of the deviatoric stress tensor s_{ij} and is defined as

$$II_s = \frac{1}{2} s_{ij} s_{ij}.$$

The abscissa, $t_{ii}/3$, represents the mean compressive stress.

The mean normal compressive stress–volumetric strain behavior of the wet sand is given in Fig. 4b that shows the variation of pressure as a function of volumetric strain for wet concrete sand with air filled voids content at a level between 1 and 5 percent. For the purposes of this work, the volumetric strain ε_v was defined as

$$\varepsilon_v = -\ln\left(\frac{V}{V_0}\right),$$

the negative value of the natural logarithm of the ratio of the current volume to the initial volume. These data were also used, in tabular form, to populate the LS-DYNA material model. The soil was modeled as having a wet density of 2145.3 kg/m^3, a Young's modulus of 7.1028 GPa, a shear modulus of 330.35 MPa, a tensile fracture cutoff pressure of −24.638 kPa, and the "fail" parameter was set to 2.

A cylindrical ALE domain geometry was chosen for this work. The cylindrical domain finite element mesh is shown in Fig. 5. The radius

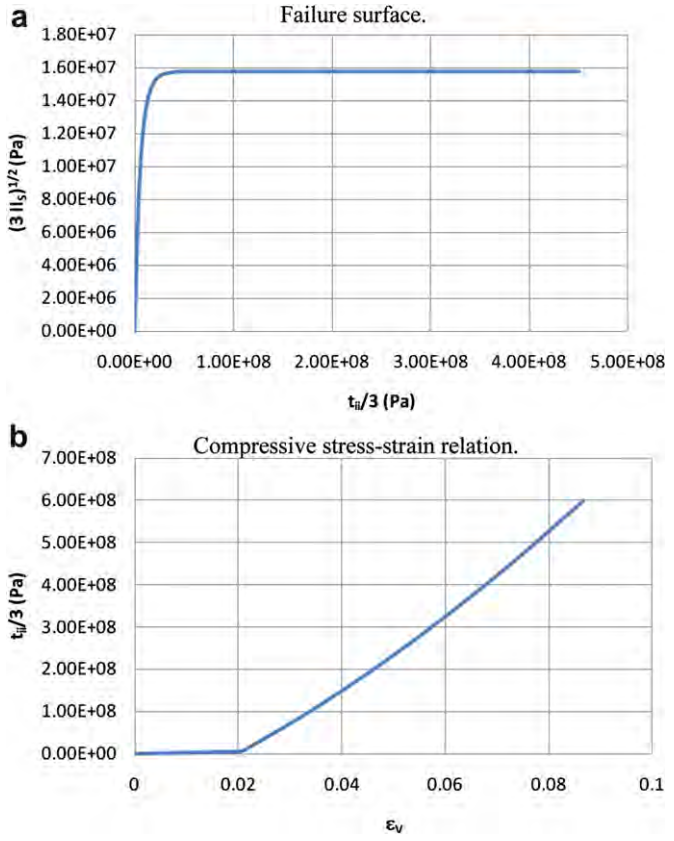

Fig. 4. a) Failure surface for wet concrete sand defined by II_s, the second invariant of the deviatoric stress tensor as a function of pressure $t_{ii}/3$. (b) Mean compressive normal stress – volumetric–strain relationship for wet concrete sand. Both are for air filled void content between 1 and 5 percent [19].

of the cylindrical ALE domain was 0.48 m. The height of the lower portion of the domain in the axial direction, which initially contained the soil and the explosive, was 164.1 mm; the height of the upper portion, initially filled by air and the rigid target, was also 164.1 mm.

The mesh size for the ALE domain was varied by radial position in the circular plane of the domain. In the region closest to the center, the mesh size was approximately 2 mm; toward the outer radius of the domain, the mesh size was about 16 mm. The distance between nodes in the vertical, axial, direction was approximately 2 mm.

LS-DYNA uses an isotropic method for the advection of quantities between elements. This means that such quantities are

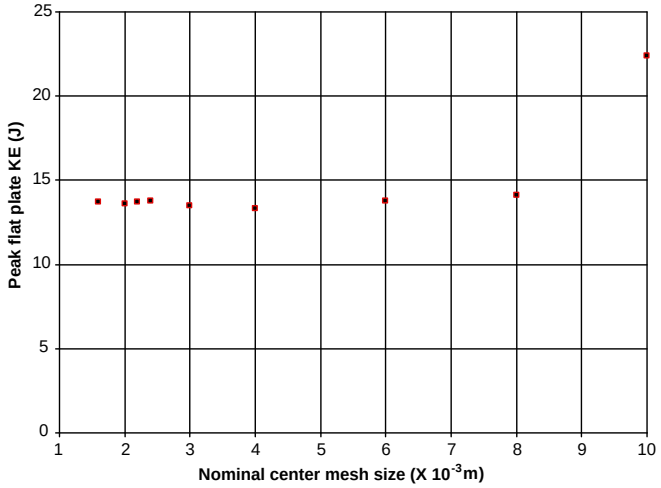

Fig. 6. Results of the mesh convergence study. The nominally 2 mm mesh that was used for the computational work was clearly in the converged region.

transported through the faces of elements but not through corners or edges [16]. For the type of physical problem treated in the present work mass, momentum, and energy are radially propagated in the plane of the cylinder. An unstructured mesh was used, therefore, in order to better match the physics of the problem.

A mesh convergence study was performed which involved excitation of the flat target by means of the explosive charge buried in wet sand directly beneath the center of the target. The results of this study indicated that the mesh with the nominally 0.002 m center region was well within the converged region (Fig. 6).

4. Results

4.1. Experimental results

A summary of the experimental results for the various targets is given in Table 1. For factor combinations for which more than one test was performed it can be seen that there was some degree of variability. Thus far no detailed examination of test-to-test variability has been performed, but possible sources for this variation might include small differences in explosive charge mass, in soil moisture content, as well as in the spatial configuration of the explosive in the soil and the height of the target above the top of the soil. An examination of the result averages reveals several trends. It was observed that, for the cases where the charge was located

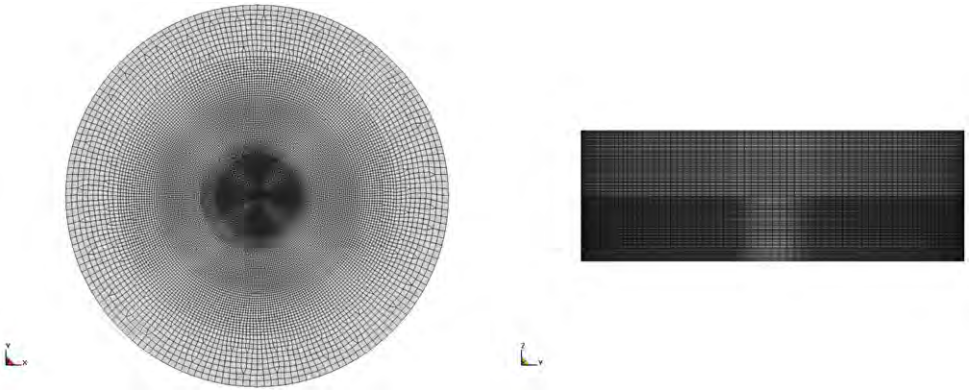

Fig. 5. The mesh that was used for the ALE computational domain.

Table 1
Computational and experimental results for center and quarter shot excitation of target plates. Negative angle definitions indicate downwardly concave targets. Positive angle definitions indicate that targets were downwardly convex. For factor combinations for which more than one test was performed, individual test results are shown first and these are then followed by their average value.

Target bottom angle [°]	Charge location	Experimentally determined impulse imparted to target [N-s]	Peak impulse imparted to target based on computation [N-s]	Percentage difference between computation and average of experimental results
−21	Center	5.62, 6.42; average: 6.02	6.50	7.7
−13	Center	6.41, 6.96, 6.66; average: 6.68	6.69	0.2
0	Center	6.49, 6.78; average: 6.64	6.64	0.0 – used to calibrate model
13	Center	5.26	5.26	0.0
21	Center	4.84	4.38	−9.5
0	Quarter	8.35, 7.44; average: 7.90	7.18	−9.1
13	Quarter	6.94	6.26	−9.8
21	Quarter	5.74	5.36	−6.6

directly beneath the centers of the targets, the amount of peak momentum imparted to the flat target and the 13° concave target were relatively similar whereas the 21° concave target exhibited a moderately lower level. For these center shots, the severity of the blast load was significantly reduced for both of the hulls that were downwardly convex, with increased reduction for the 21° hull.

The nominal depth of burial of the explosive and the stand-off distance between the targets and the upper surface of the soil bed was the same for all of the tests performed for this work. The target stand-off distance was taken to be the vertical distance from the sand surface to the nearest point on the target. For the downwardly convex targets, this point was at the lateral centerline of plate. For the downwardly concave targets, these points were at the outer edges of the plate. As a result, the distance between the surfaces of the angled plates and the charge was greater than it was between the flat plate and the charge.

Fig. 7 shows experimental results for a flat plate excited by a 4.4-g charge with a depth of burial of 5.34 mm in wet sand. It can be observed that impulse decreases significantly with increasing stand off distance. It seems most likely that at least some of the observed reduction in the loading of the 21 degree downwardly concave, the 13 degree downwardly convex, and the 21 degree downwardly convex plates was a result of the increased distance between explosive and target. It is interesting to note that the downwardly convex targets, for the case of central loading, exhibited lower momentum than did the downwardly concave targets (Table 1).

In order to more carefully examine the mechanics of target loading as it relates to angled surfaces, a series of tests was conducted that involved the measurement of specific impulse at various locations on rigid downwardly convex targets as well as on rigid flat plates. For this work measurements were taken, using high-speed digital video, of the impulse delivered to tapered, removable 25.4 mm diameter plugs. The mass of the plugs was varied, depending on the location on the rigid target, so that the velocity could be most accurately measured. Results from this work are shown in Fig. 8.

Referring to Fig. 8, it is difficult, for distances greater than about 50 or 60 mm from the explosive, to distinguish between the response of the flat plate and the angled plate. However, as the distance between the explosive and the target decreased below this level there was some divergence between the results for the two cases. As the distance decreased, there appeared to be a trend toward higher excitation of the flat plate than of the angled target. On this basis it could be hypothesized that some portion of the reduction in excitation was a result of the effect of the geometric shape of the bottom of the target. The performance of additional tests at smaller distances between charge and flat plate would help to clarify whether such an hypothesis is, in fact, correct. A comparison, taken from high-speed video of some of the blast experiments, of the response of plates to excitation beneath their centerline and for quarter shots, i.e., for shots with charge located beneath a position halfway between the center and the outer lateral edge of the targets, can be seen in Fig. 9. These images, from high-speed video recordings of the blast events, were taken 20 ms after explosive detonation.

For the impacts that involved flat and downwardly convex plates (Table 1), the imparted momentum was higher for shots with the charge located halfway between the center and edge of the target than it was for the case of the centerline shots. This was a result of the combination of two factors. First, a significant rotational

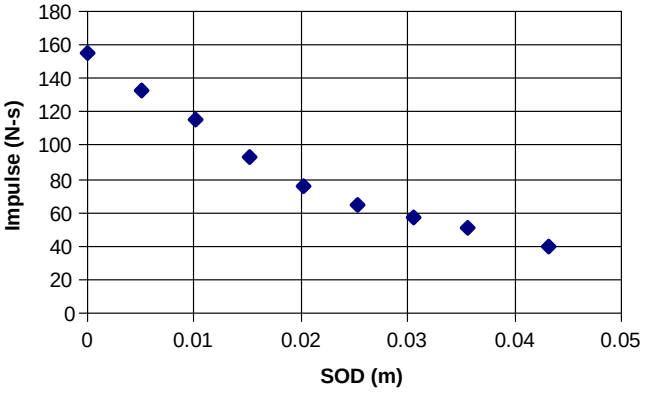

Fig. 7. Impulse versus stand off distance (SOD) for flat plate targets. Charge size was 4.4 g and depth of burial was 5.34 mm. Impulse decreased exponentially with increasing distance between explosive and flat plate target.

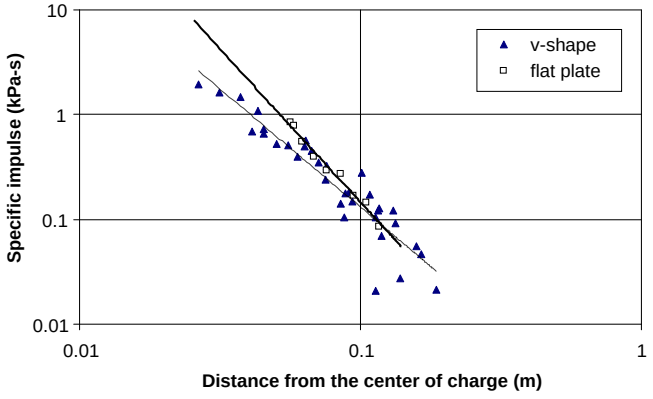

Fig. 8. Specific impulse versus radial distance from explosive charge center as measured by the momentum of tapered plugs located at various positions on flat and downwardly convex rigid aluminum targets.

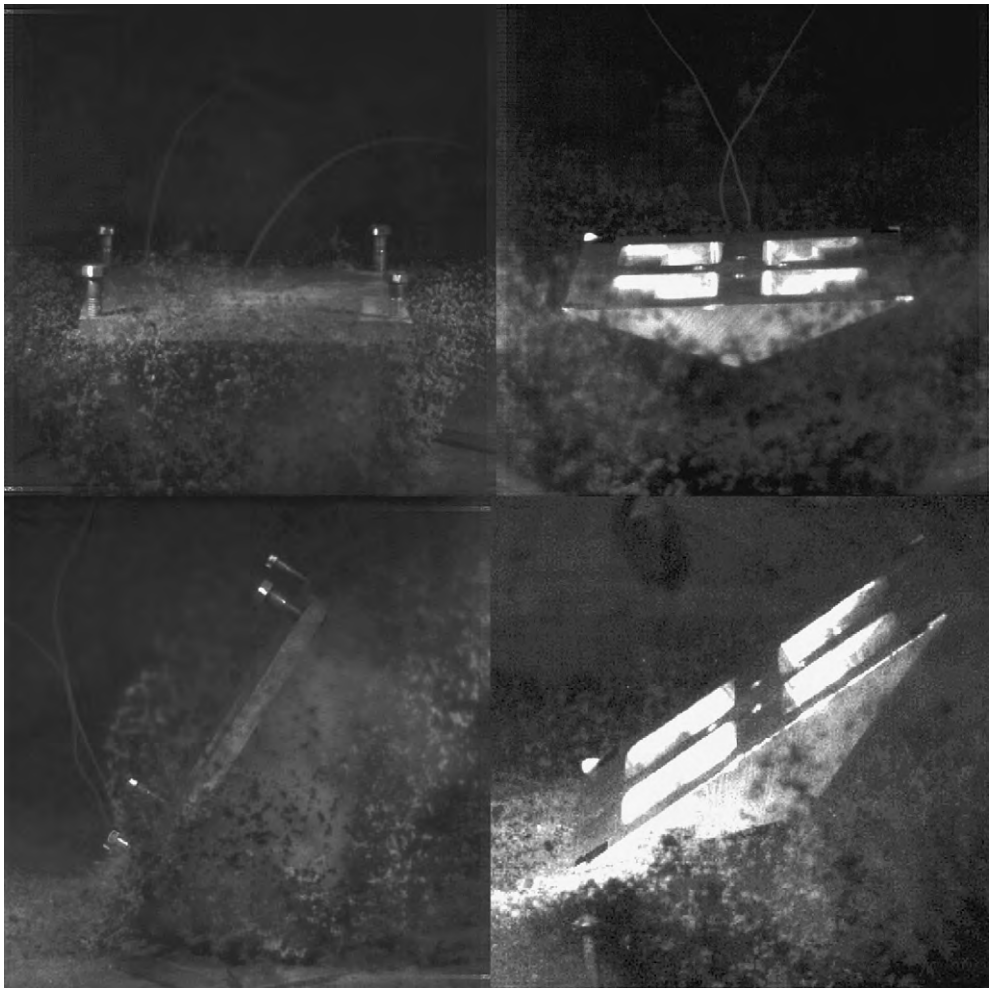

Fig. 9. Conformation of flat (left), and 21° convex down (right) plates 20 ms after charge detonation. Top row: targets that were excited by means of explosive buried beneath target centerline. Bottom row: targets that were excited by means of buried explosive charge located halfway between the centerline and outer lateral edge of target.

component of the motion was caused by the offset location of the bottom surfaces of the targets relative to the progression of the blast front. This effect for the offset explosive location, developed from computational results, is shown in Fig. 10. Fig. 10a shows the initial configuration of the flat plate as it rests upon its supports. Fig. 10b shows the conformation of the plate about 200 μs after the initiation of the detonation, at which point it is constrained on its left side by the support bolt but is rotating counter-clockwise and separating slightly on its right side from support bolt. Fig. 10c shows the target 8 ms after detonation, rotating counter-clockwise and completely separated from the bolt supports. A hand calculation for impulsive loading of a very thin, rigid rod helped us to more fundamentally grasp the reasons that the offset shots resulted in higher target translational momentum than did the center shots. If an impulse is defined as, say [$\delta(t)$ FC] where $\delta(t)$ is the Dirac delta function and FC is the magnitude of the impulsive load then it can be shown, by integrating the relations for conservation of linear and angular momentum, that this impulse applied as quarter loading to the rod will impart 1.75 times the kinetic energy that it would impart if applied at the center of the rod. Therefore, even a somewhat lower impulsive load applied as a quarter shot could still impart more kinetic energy to a target than a somewhat higher impulsive load applied at the center of the target.

In addition, the initial constraint on the targets caused by the presence of the bolts used to position the targets above the top surface of the soil served to redirect a portion of the quarter shot rotational kinetic energy to the end that it was converted to translational kinetic energy thereby increasing the translational momentum of the targets' centers of mass. This point is illustrated in Fig. 11, taken from a comparison of computational results for the

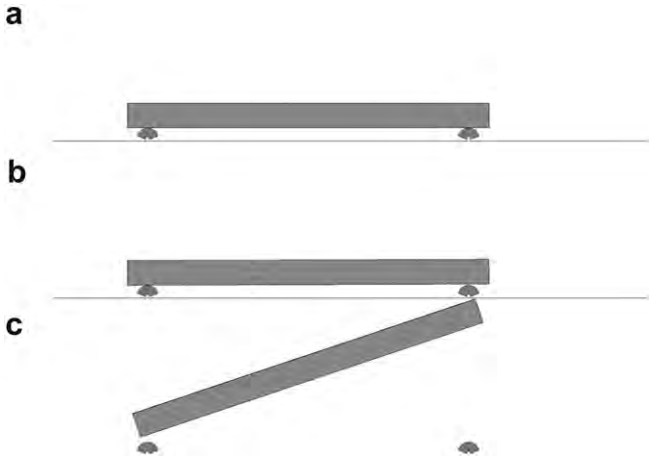

Fig. 10. Effect, for quarter shot computations, of constraining bolt supports on target dynamics. (a) Target in initial configuration. (b). Target 200 μs after detonation, constrained on left side by support bolt but rotating and separating slightly on right side from support bolt. (c) Target 8 ms after detonation, rotating and separated from all bolt supports.

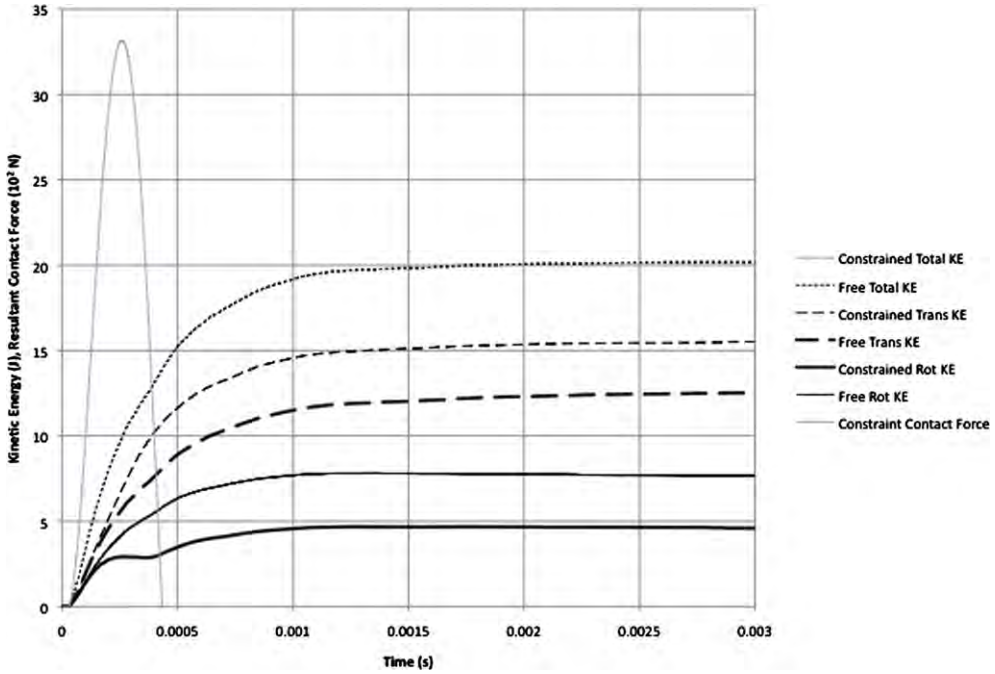

Fig. 11. Computational kinetic energy results for flat plate rotation constrained by support bolts are compared with results for unconstrained flat plate. Support bolt constraint contact forces, for the constrained case, are superimposed.

flat plate with offset excitation but in one case constrained by the support bolts and, in another case floating free in space, that is, with no bolt constraints. The total calculated kinetic energy for the target is almost the same for the constrained case as it is for the unconstrained case. However, it can be seen that the partitioning of rotational and translational energy is significantly different for the two cases. In the constrained case, the torque resulting from the contact forces between the target and the constraining bolts results in a significant reduction of target rotational inertia, and therefore, rotational kinetic energy, which leads to a higher proportion of target translational kinetic energy – and translational momentum – than that which is observed for the unconstrained case. It is interesting to note the correspondence between the constrained case contact forces and the rotational kinetic energy of the target for the constrained case.

4.2. Computational results

Test data available from the SABER code [19] were used for building soil models with 1 percent air filled void and 5 percent air filled void wet concrete sand. Computations performed using models for these two soils for the case of the flat plate and centerline location of the explosive produced target peak momentum of 8.07 N-s and 5.24 N-s, respectively. One of the primary aims of this study was to examine the use of a computational method that would be based very much on the physics of the problem and that would involve a minimal amount of tuning of model parameters. However, no test data were immediately available for concrete sand water levels that correlated to values between 1 percent and 5 percent air filled voids. As a result, an iterative process, based on the physical behavior of the soil, was used to develop interpolated values for the various components of the soil model to the end that the computational model produced a peak target momentum that matched the experimental peak level of 6.64 N-s. Computed target momentum – time histories generated using concrete sand models with 1 percent, 5 percent, and the calibrated intermediate level of air filled voids are presented in Fig. 12.

High speed video was used by Genson [7] in order to investigate the evolution, for time increments of 40 μs, of the blast for the case of a 0.636-g explosive charge, wet sand, 4.826 mm depth of charge burial but with no target, in other words, under the same conditions of soil and explosive that were used in the present study for aluminum target excitation. Computations, using the ALE method described above, were performed for this same set of parameters. A comparison of these results is given in Fig. 13. All frames in the figure are shown at the same scale. In the figure, the soil was represented by the light gray colored continuum while the reaction products from the detonation of the explosive were represented in

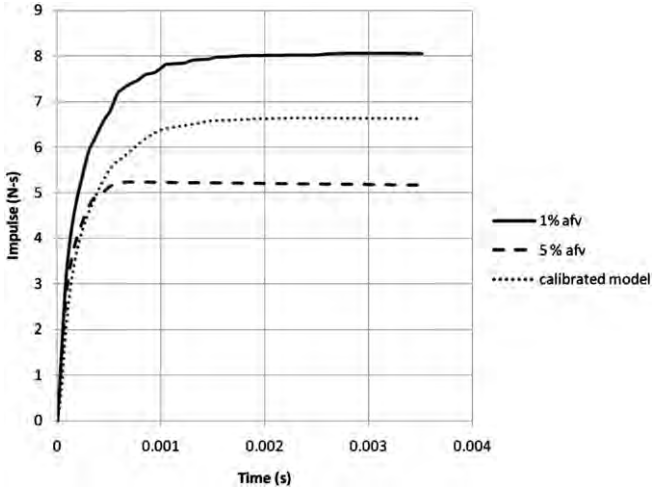

Fig. 12. Computed target momentum – time histories generated using concrete sand models with 1 percent, 5 percent, and a calibrated, intermediate level of air filled voids for the case of the flat plate with explosive charge buried directly beneath the lateral centerline of the plate.

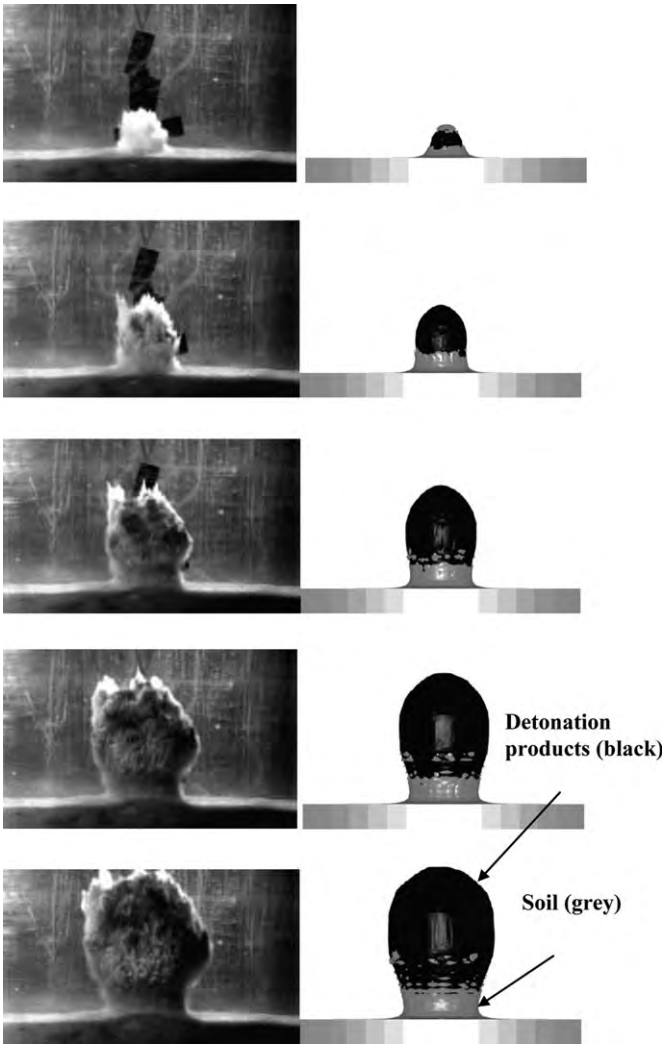

Fig. 13. Forty microseconds per frame comparison of experimental results (from Genson [7]), on the left, with computational results, on the right, for the case of no target, 0.636 g charge size, and 4.826 mm depth of charge burial in wet sand. In the animation illustrations, the grey material is the wet sand; the black material is the detonation reaction product gases.

black. As a result of the relatively low volume fraction of sand in the dust cloud and the computational mesh size in comparison to the scale of the sand particles, it was not possible to capture, for the case of the computations, some of the fine detail of the dust that comprised the cloud of ejecta.

During the course of computations performed on the downwardly convex target plates for center shot charge location, convergence problems emerged for the case of the 250 mm computational domain radius. A physically unrealistic continuous increase in target momentum was observed in the plate response to the blast load. This was caused by the emergence of numerical instabilities at the ALE computational domain boundaries. A convergence study that involved several iterations with expansion of the outer radius of the cylindrical ALE computational domain beyond its initial value of 246.3 mm supported this hypothesis. Based on the results of the convergence study, the computational domain size was ultimately expanded to a radius of 480 mm.

Computations were performed first for center shots on all target configurations. A primary objective of the computational work was to determine whether it would be possible to match the experimental results for the rigid plates by using ALE computations and the soil model described above, a soil model that was based purely on quasi-static determination of the soil behavior. The results from these computations are compared with the experimental findings in Table 1. Percentage difference was calculated based on the deviation of computational results from experimental results. The case of the flat plate, center charge location was used to calibrate the soil model. Thus, for that particular case, the calculation of percentage difference was not relevant. It can be seen that, for the remaining cases, the agreement between computation and experiment was reasonable.

Computations were also performed for some of the cases that involved explosive buried halfway between the center and the outside lateral edge of these targets. The results of these calculations are shown in Table 1. The agreement with the experimental results was found to be, for these cases, also very good.

6. Summary and conclusions

The response of downwardly convex, flat, and downwardly concave rigid targets to excitation from shallow buried explosives located at various locations beneath the targets was examined using an approach that involved experimental as well as computational methods. High-speed video techniques were used to observe blast phenomena and measure the dynamics of the target plates. An arbitrary Langrangian–Eulerian (ALE) treatment was used to model the mechanics of the explosive, soil and air. The two-way coupling between the fluid and solid constituents of the problem was handled computationally by means of a penalty contact method.

It was observed experimentally that hulls – with bottom geometries that were both downwardly convex – reduced the amount of momentum imparted to the target by the explosive detonation products and the soil. Also, it was observed that the rotational effects imparted to flat and downwardly convex targets with explosive buried in non-centerline locations were significant and clearly invite further examination. The computations that were performed were found to agree very closely with experimental results. Thus the hypothesis that a computational soil model, based purely on quasi-static test evaluations, could enable such close agreement between experiment and computational results was supported by the work that was performed for this study.

Acknowledgements

The authors wish to thank Leslie Taylor from the University of Maryland, Chian-Fong Yen, Scott Kukuck, and Douglas Kooker from the US Army Research Laboratory as well as Erin Williams, Kent Danielson, Jon Windham, and Steve Akers from the US Engineer Research and Development Center for various insights with regard to the interaction of soils and shallow buried explosives. The authors are also grateful to the US Army Tank-Automotive Research, Development and Engineering Center and the Center for Energetic Concepts at the University of Maryland for the support they provided for this work.

References

[1] Baker WE. Explosions in air. Austin: University of Texas Press; 1973.
[2] Kinney GF, Graham KJ. Explosive shocks in air. New York: Springer Verlag; 1985.
[3] Westine PS, Morris BL, Cox PA, Polch E. Development of a computer program for floor plate response from land mine explosions. Contract report no. 13045. U.S. Army TACOM Research and Development Center; 1985.
[4] Fourney WL, Leiste U, Bonenberger R, Goodings D. Explosive impulse on plates. Fragblast 2005;9(1):1–17.
[5] Taylor LC, Skaggs RR, Gault W. Vertical impulse measurements of mines buried in saturated sand. Fragblast 2005;9(1):19–28.

[6] Taylor LC, Fourney WL, Leiste U, Genson K. Geometrical shaping of vehicles for reducing impulse from buried explosions. In: Joint classified bombs/warheads & ballistics symposium, Monterey, CA, 2008.
[7] Genson K. Vehicle shaping for mine blast damage reduction, M.S. thesis. College Park: University of Maryland, 2006.
[8] Laine L, Sandvik A. Derivation of mechanical properties for sand. In: 4th Asia-pacific conference on shock and impact loads on structures. Singapore; 2001.
[9] Szymczak W. Platform loading from explosions in saturated sand using a visco-plastic model. Fragblast 2005;9(4):189–203.
[10] Grujicic MB, Pandurangan B, Cheeseman BA. The effect of degree of saturation of sand on detonation phenomena associated with shallow-buried and ground-laid mines. Shock and Vibration 2006;13:41–62.
[11] Grujicic M, Pandurangan B, Qiao R, Cheeseman BA, Skaggs RR, Gupta R. Parameterization of the porous-material model for sand with different levels of water saturation. Soil Dynamics and Earthquake Engineering 2008;28:20–35.
[12] Deshpande VS, McMeeking RM, Wadley HNG, Evans AG. Constitutive model for predicting dynamic interactions between soil ejecta and structural panels. Journal of the Mechanics and Physics of Solids 2009;57(8):1139–64.
[13] Neuberger A, Peles S, Rittel D. Scaling the response of circular plates subjected to large and close-range spherical explosions. Part II: buried charges. International Journal of Impact Engineering. 2007;34:874–82.
[14] Williams EM, Windham JE, Ehrgott JQ, Danielson KT, Gorsich TJ. Effect of soil properties on an above ground blast environment from buried bare charges. In: 20th military aspects of blast and shock symposium, Oslo, Norway, 2008.
[15] Souli M. LS-DYNA advanced course in ale and fluid/structure coupling. Livermore, CA: Livermore Software Technology Corporation; 2004.
[16] Hallquist JO. LS-DYNA theoretical manual. Livermore, CA: Livermore Software Technology Corporation; 2006.
[17] Du Bois P, Schwer L. LS-DYNA modeling of blast and penetration. Livermore, CA: Livermore Software Technology Corporation; 2007.
[18] Chen WF, Baladi GY. Soil plasticity: theory and implementation. New York: Elsevier Science; 1985.
[19] Zimmerman HD, Shimano RT, Ito YM. Early-time ground shock from buried conventional explosives: user's guide for SABER-PC/CWE, WES IR SL-92-1. Vicksburg, MS: U.S. Army Corps of Engineers, Waterways Experiment Station; 1992.

NO. OF COPIES	ORGANIZATION
1 (PDF only)	DEFENSE TECHNICAL INFORMATION CTR DTIC OCA 8725 JOHN J KINGMAN RD STE 0944 FORT BELVOIR VA 22060-6218
1	DIRECTOR US ARMY RESEARCH LAB IMNE ALC HRR 2800 POWDER MILL RD ADELPHI MD 20783-1197
1	DIRECTOR US ARMY RESEARCH LAB RDRL CIO LL 2800 POWDER MILL RD ADELPHI MD 20783-1197
1	DIRECTOR US ARMY RESEARCH LAB RDRL CIO MT 2800 POWDER MILL RD ADELPHI MD 20783-1197
1	DIRECTOR US ARMY RESEARCH LAB RDRL D 2800 POWDER MILL RD ADELPHI MD 20783-1197

INTENTIONALLY LEFT BLANK.